New Possibilities with Sobolev Active Contours*

Ganesh Sundaramoorthi[1], Anthony Yezzi[1], Andrea C. Mennucci[2], and Guillermo Sapiro[3]

[1] School of Electrical Engineering, Georgia Institute of Technology, Atlanta, USA
[2] Scuola Normale Superiore, Pisa, Italy
[3] Dept. of Electrical & Computer Engineering, University of Minnesota, Minneapolis, USA

Abstract. Recently, the Sobolev metric was introduced to define gradient flows of various geometric active contour energies. It was shown that the Sobolev metric out-performs the traditional metric for the same energy in many cases such as for tracking where the coarse scale changes of the contour are important. Some interesting properties of Sobolev gradient flows are that they stabilize certain unstable traditional flows, and the order of the evolution PDEs are reduced when compared with traditional gradient flows of the same energies. In this paper, we explore new possibilities for active contours made possible by Sobolev active contours. The Sobolev method allows one to implement new energy-based active contour models that were not otherwise considered because the traditional minimizing method cannot be used. In particular, we exploit the stabilizing and the order reducing properties of Sobolev gradients to implement the gradient descent of these new energies. We give examples of this class of energies, which include some simple geometric priors and new edge-based energies. We will show that these energies can be quite useful for segmentation and tracking. We will show that the gradient flows using the traditional metric are either ill-posed or numerically difficult to implement, and then show that the flows can be implemented in a stable and numerically feasible manner using the Sobolev gradient.

1 Introduction

Active contours [1] is a popular technique for the segmentation problem. Over the years there has been a progression of active contours derived from edge-based energies (*e.g.*, [2,3]), to region-based energies (*e.g.*, [4,5]), to more recently, prior-based energies (*e.g.*, [6,7,8]) and energies incorporating complex geometrical information (*e.g.*, [9,10,11]). The progression from simple to more complicated energies is not only due to a desire to segment more complicated images, but it can also be attributed to the traditional gradient descent technique becoming trapped by (undesirable) local minima of the energy being optimized. Therefore there have been efforts to design optimization schemes that can obtain the global minimum curve of a generic energy. For example, the minimal path technique [12] was designed to find the global minimal solution of the edge-based energy considered in [2,3]. Another technique, called graph cuts [13,14], was designed for minimizing discrete approximations to some active contour energies.

* G. Sundaramoorthi and A. Yezzi were supported by NSF CCR-0133736, NIH/NINDS R01-NS-037747, and Airforce MURI; G. Sapiro was partially supported by NSF, ONR, NGA, DARPA, and the McKnight Foundation.

F. Sgallari, A. Murli, and N. Paragios (Eds.): SSVM 2007, LNCS 4485, pp. 153–164, 2007.

The limitation of these global methods is that they may be applied to only certain types of energies, and therefore gradient descent methods must be used in many cases. Recently, [15,16] have noticed that the gradient of an energy that is used in descent algorithms depends on a metric chosen on the space of curves. This fact has been ignored in previous active contour literature; indeed previous active contours were always derived from the geometric $\mathbb{L}^2$-type (H^0) metric. Accordingly, [17,18] have considered new metrics in the space of curves. It was shown that the metric choice affects the path taken to minimize an energy, and that certain local minima of an energy can be avoided by designing an appropriate metric. In particular, Sobolev metrics were considered. It was shown that gradient flows according to Sobolev metrics give smooth global flows, which avoid many local minima of energies that trap the usual $\mathbb{L}^2$ gradient flow. In [19], it was shown that Sobolev active contours move successively from coarse to finer scale motions, and therefore the method is suitable for tracking.

The main purpose of [17,19] was to show advantages of using Sobolev active contours over the traditional active contour based on the same energy. In contrast, in this paper we introduce *new* active contour energies that are quite useful for various segmentation tasks, but *cannot* be minimized with the traditional $\mathbb{L}^2$ active contour (nor other global optimization techniques), and the Sobolev active contour must be used. We show a few examples of these energies, which include simple geometric priors for active contours and new edge-based energies. These new energies fall into two categories: one in which the resulting $\mathbb{L}^2$ flows are not stable, and another in which the traditional gradient flow results in high order PDEs that are numerically difficult to implement using level set or particle based methods. We propose to use Sobolev active contours, which avoid both of these problems.

This paper is meant to illustrate that energies that result in $\mathbb{L}^2$ unstable or high order flows can still be considered for optimization with the Sobolev method (and these energies need not be discarded or adjusted). As such we give a few simple examples of the energies that fall into these categories. Experiments in this paper show the types of behaviors that can be obtained from the simple energies considered, and one can obtain good results on more complex images by combining these results with other energies.

The graph cut method is known to be able to minimize three types of geometric energies: weighted length, flux of a vector field, and weighted area [14]. Some of the energies we consider are non-simple operations (such as division) of the previous energies mentioned, and the technique in [14] does not apply; indeed we are not certain that a graph for the energies we consider can be constructed. Other energies we consider have curvature inside the integral; since edge weights in graph cuts depend on an edge (between a pixel and its neighbor), it is unclear whether a curvature term may be incorporated in the framework since to compute curvature one needs three points. In any case, since graph cut methods do not have sub pixel accuracy, curvature computations would be extremely inaccurate.

In [18], the authors consider various different metrics resulting in 'coherent' gradient flows; indeed they construct flows that favor certain group motions such as affine motions. In the case of the affine group (others are analogous), the flow is formed by re-weighting the affine component of the traditional gradient higher and the component orthogonal (according to the $\mathbb{L}^2$ inner product) lower. For the class of energies

that we wish to explore in this paper however, the metrics proposed by [18] based on group motions also suffer from the same problems as the traditional $\mathbb{L}^2$ metric; namely, these flows are either not stable or are high order PDEs and are difficult to implement numerically.

2 Some Useful Energies Precluded by $\mathbb{L}^2$

In this section, we introduce three geometric "energies", which can be used as building blocks to produce a variety of other useful energies (to be described in subsequent sections). We then derive the $\mathbb{L}^2$ gradient and show that the gradient descent flow is either ill-posed or very difficult to implement numerically. We then derive the Sobolev gradient flows, and justify that they are well-posed and numerically feasible to implement.

Before we proceed, we introduce the notation used in this paper. A contour will be denoted, c; its length is L. We define $\overline{\cdot} := L^{-1}\int_c \cdot\, \mathrm{d}s$, where $\mathrm{d}s$ is the arc length measure of c. Throughout this paper, we define the Sobolev metric as $\|h\|^2_{\text{Sobolev}} := |\overline{h}|^2 + \lambda\|h'\|^2_{\mathbb{L}^2}$, where h is a perturbation of c, h' is the arc parameter derivative, and $\lambda > 0$ is a scaling factor. We note the fact from [17] that the Sobolev gradient can be computed from the $\mathbb{L}^2$ gradient as $\nabla_{\text{Sobolev}} E = K * \nabla_{\mathbb{L}^2} E$, where $*$ is circular convolution and K is a kernel found in [17] whose second derivative exists in a distributional sense.

The first "energy" that we introduce is the following generalization of average weighted length:

$$E(c) = \frac{1}{L}\int_c \phi(c(s))\,\mathrm{d}s = \overline{\phi}, \tag{1}$$

where $\phi : \mathbb{R}^2 \to \mathbb{R}^k$ where $k \geq 1$. The $\mathbb{L}^2$ gradient of this energy is

$$\nabla_{\mathbb{L}^2} E(c) = \mathcal{N}[\mathcal{N}^T (D\phi)^T - \kappa(\phi - \overline{\phi})^T] \tag{2}$$

where T denotes transpose, and D denotes derivative. Since $\phi - \overline{\phi}$ is not strictly positive, the gradient descent flow has a component that is reverse heat flow on half of the contour, and therefore the $\mathbb{L}^2$ gradient descent is ill-posed. Note that the reverse heat component attempts to increase the length of certain portions of the contour. Since the ill-posedness of the $\mathbb{L}^2$ flow only arises from the length increasing effect, we expect the Sobolev gradient flow to be well-posed. This is because increasing the length of the contour is a well-posed process using the Sobolev gradient; indeed, the Sobolev gradient ascent for length is simply a rescaling of the contour [17]. Computing the Sobolev gradient of (1) we have

$$\nabla_{\text{Sobolev}} E(c) = -\frac{c - \overline{c}}{\lambda L^2}\overline{\phi}^T + K * (D\phi)^T + K' * (c_s \phi^T) \tag{3}$$

Notice that the component, $\mathcal{N}\overline{\phi}^T\kappa$, of the $\mathbb{L}^2$ gradient that caused the ill-posedness has been converted to the first term of the Sobolev gradient (3), which is a stable rescaling of the contour.

Next, we introduce a scaled version of the weighted area, given by the energy

$$E(c) = \frac{1}{L^2}\int_R \phi(x)\,\mathrm{d}A(x) = \frac{A_\phi}{L^2}, \tag{4}$$

where $\phi : \mathbb{R}^2 \to \mathbb{R}$, R is the region enclosed by c, and $\mathrm{d}A$ is the area measure in $\mathbb{R}^2$. Similar to the previous energy, the ill-posedness of the $\mathbb{L}^2$ gradient descent flow of (4) is due to the scale factor of L^{-2}, which causes a length increasing component in the gradients, and is ill-posed with respect to $\mathbb{L}^2$. Indeed, calculating the gradient, we have

$$\nabla E(c) = \frac{L^2 \nabla A_\phi - 2A_\phi L \nabla L}{L^4} = \frac{A_\phi}{L^2}\left[\frac{\nabla A_\phi}{A_\phi} - 2\frac{\nabla L}{L}\right].$$

Therefore, we see that

$$\nabla_{\text{Sobolev}} E(c) = -\frac{A_\phi}{L^2}\left[L\frac{K * (\phi\mathcal{N})}{A_\phi} + 2\frac{c - \overline{c}}{\lambda L^2}\right], \tag{5}$$

which leads to a well-posed descent (and ascent).

Lastly, we introduce the following generalization of the elastic energy:

$$E(c) = L\int_c \phi(c(s))\kappa^2(s)\,\mathrm{d}s, \tag{6}$$

where $\phi : \mathbb{R}^2 \to \mathbb{R}$, and κ is the signed curvature of c. The factor of L multiplying the integral makes the energy scale-invariant when ϕ is a constant. Note that without the L factor, one can make the elastic energy arbitrarily small by scaling a contour large enough. We will also consider the scale-varying elastic energy without the L. These energies have been used in the past for the "curve completion" problem, which is a curve interpolation problem between two points [20,21]. In [21], for the numerical implementation, a discrete version of the energy is minimized with a "shooting" method. One can show that the $\mathbb{L}^2$ gradient of (6) is

$$\nabla_{\mathbb{L}^2} E(c) = -Ec_{ss} + 2L^2\partial_{ss}(\phi c_{ss}) + 3L^2\partial_s(\phi\kappa^2 c_s) + L^2\kappa^2\nabla\phi \tag{7}$$

We note the result of [22], which considers the $\mathbb{L}^2$ gradient descent flow of an energy similar to (6). The author of [22] considers the $\mathbb{L}^2$ gradient descent flow of the energy

$$E(c) = \int_c (\kappa^2(s) + \alpha)\,\mathrm{d}s$$

where $\alpha > 0$. It is proven that an immersed/regular curve evolving under this fourth-order flow stays immersed/regular, and a solution exists for all time. In the case when ϕ is a constant, the flow (7) is similar to the flow that is considered in [22], except that α is time varying in (7). For numerical implementation, the fourth order flow (7) is difficult to implement with marker particle methods because of numerical artifacts arising from fourth order differences, and it is even more problematic to implement with level set methods because the flow is not known to have a maximum principle and because of numerical artifacts. These are the reasons for considering the Sobolev gradient:

$$\nabla_{\text{Sobolev}} E = -\frac{E}{\lambda L^2}(\overline{c} - c) + \frac{2}{\lambda}(\overline{(\phi\kappa\mathcal{N})} - \phi\kappa\mathcal{N}) - 3L^2K' * (\phi\kappa^2\mathcal{T}) + L^2K * (\kappa^2\nabla\phi). \tag{8}$$

The Sobolev flow is second order, although it is a integral PDE. We can bypass the question about a maximum principle for this flow since the local terms have a maximum principle, and we perform extensions in the level set implementation for global terms.

3 Geometric Priors for Active Contours

In this section, we introduce some simple geometric shape priors for use in active contour segmentation. As these energies are formed from the energies presented in the previous section, they cannot be minimized with the usual $\mathbb{L}^2$ gradient descent.

3.1 Length and Smoothness Priors

In many active contour models, a curvature term, *i.e.*, $\alpha\kappa\mathcal{N}$ (where $\alpha > 0$ is a weight), is added to a data-based curve evolution. The resulting flow will inherit regularizing properties such as smoothing the curve from the addition of this term. If the active contour model is based on minimizing an energy, then adding a curvature term is equivalent to adding a length penalty to the original energy, that is, if E_{data} is the original energy then the new energy being optimized (w.r.t the traditional $\mathbb{L}^2$ metric) is

$$E(c) = E_{\text{data}}(c) + \alpha L(c). \tag{9}$$

This may be considered as a simple prior in which we assume that the length of the curve is to be shrunk. In general segmentation situations, this assumption may not be applicable. A more general energy incorporating length information, when such prior length information is known, is

$$E(c) = E_{\text{data}}(c) + \alpha(L(c) - L_0)^2, \tag{10}$$

in which it is assumed that length of the target curve is near L_0. See [23] (and references within) for related flows where the length of the curve is preserved. Note that this prior allows for increasing or decreasing the length of the curve based on the current length of the curve and the value of L_0. The $\mathbb{L}^2$ gradient is

$$\nabla_{\mathbb{L}^2} E(c) = \nabla_{\mathbb{L}^2} E_{\text{data}}(c) - 2\alpha(L - L_0)\kappa\mathcal{N},$$

which leads to an unstable flow if $L - L_0 < 0$. The Sobolev gradient is

$$\nabla_{\text{Sobolev}} E(c) = \nabla_{\text{Sobolev}} E_{\text{data}}(c) + 2\alpha(L - L_0)\frac{c - \overline{c}}{\lambda L},$$

which is stable if the data term is stable.

In active contour works, the goal of adding the length penalty may have been mainly for obtaining the regularizing properties of the resulting flow, even though the energy itself does not favor more regular curves. It is evident that the Sobolev length descent does not regularize the active contour since the flow is a rescaling of the curve. Thus, to introduce smoothness into the Sobolev active contour (and even the $\mathbb{L}^2$ active contour), we introduce the smoothness prior given by the energy,

$$E(c) = E_{\text{data}}(c) + \alpha L(c) \int_c \kappa^2(s)\, \mathrm{d}s. \tag{11}$$

The energy itself favors smoother contours, and we are not relying on the properties of a particular metric for regularity; it is inherent in the energy itself. The factor of L is for scale-invariance (unlike the length descent, this regularizer does not favor shrinking the length of the contour). Using the scale-varying and scale-invariant elastic energies as smoothness measures for active contours is mentioned but not implemented in [24,25].

3.2 Centroid and Isoperimetric Priors

We now consider incorporating prior information on the centroid, length, and area of a curve into active contour segmentation. We consider the energy

$$E(c) = E_{\text{data}}(c) + \alpha\|\overline{c} - v\|^2 + \beta(L - L_0)^2 + \gamma(A - A_0)^2 \tag{12}$$

where $\alpha, \beta, \gamma \geq 0$ are weights, $\overline{c}$ is the centroid of the curve c, $v \in \mathbb{R}^2$ is the centroid known *a-priori* (see Section 5.2 for an example of how this may be obtained), L_0 and A_0 are the prior values for the length and area. If detailed information is not known about the length and area, then that part of the energy may be replaced by the energy

$$E(c) = E_{\text{data}}(c) + \alpha\|\overline{c} - v\|^2 + \beta(\rho(c) - \rho_0)^2 \tag{13}$$

where

$$\rho(c) = \frac{A(c)}{L^2(c)} \tag{14}$$

is the isoperimetric ratio, which is a geometric measure of the relative relation between the length and area of a curve. Note that ρ is scale-invariant. It is a well known fact that the isoperimetric ratio is maximized by circles, and the maximum ratio is $1/(4\pi)$. Thus, the prior ratio must be constrained so that $\rho_0 \leq 1/(4\pi)$. Note that a low (near zero) isoperimetric ratio can be obtained by a snake-like shape, and a high ratio implies a shape that looks close to a circle. The isoperimetric ratio is mentioned to be used as a smoothness measure in [24], but this idea is not pursued.

Note that both the $\mathbb{L}^2$ gradient descents for the centroid constraint and the isoperimetric penalties are ill-posed. The isoperimetric ratio is a special case of (4) (when $\phi = 1$), and the constraint gives a gradient of $(\rho - \rho_0)\nabla\rho$, which gives an unstable $\mathbb{L}^2$ gradient descent flow when $\rho > \rho_0$. Note that the centroid is a special case of (1) (when $\phi : \mathbb{R}^2 \to \mathbb{R}^2$ is $\phi(x) = x$). The gradient of the centroid penalty is $\nabla(\overline{c})(\overline{c} - v)$, which gives an $\mathbb{L}^2$ gradient of

$$[(\overline{c} - v) \cdot \mathcal{N} - (c - \overline{c}) \cdot (\overline{c} - v)\kappa]\mathcal{N}$$

using (2). The gradient descent is unstable when $(c - \overline{c}) \cdot (\overline{c} - v) < 0$. The Sobolev gradient using (3) is

$$(\overline{c} - v) + K' * [c_s(c - \overline{c}) \cdot (\overline{c} - v)].$$

One possible use for (12) and (13) is in tracking applications (see Section 5.2).

4 New Edge-Based Active Contour Models

The energy for the traditional edge-based technique [2,3] (called geodesic active contours) is

$$E(c) = \int_c \phi(c(s))\,\mathrm{d}s \tag{15}$$

where $\phi : \mathbb{R}^2 \to \mathbb{R}$ is chosen low near edges (a common example is $\phi = 1/(1 + \|\nabla(G * I)\|)$ where G is a Gaussian smoothing filter). There are several undesirable features of

this model (even if a perfect edge-map ϕ is chosen). The energy has trivial (undesirable) minima and even minima that are not at the edges of the image (see for example [26]). This is in part due to the bias that the model has in preferring shorter length contours, which may not always be beneficial. Therefore, we propose new edge-based models.

4.1 Non-shrinking Edge-Based Model

We propose to minimize the following non-length shrinking edge-based energy:

$$E(c) = \int_c \phi(c(s)) \left(L^{-1} + \alpha L \kappa^2(s) \right) \, \mathrm{d}s, \tag{16}$$

where $\alpha \geq 0$, which we claim alleviates some of the undesirable properties of (15). An energy, which is similar to (16) (except for the factor of L on the curvature term), is considered by [27], but a discrete version of the energy is used for implementation. The first term, $\frac{1}{L} \int_c \phi \, \mathrm{d}s$ (*i.e.*, (16) when $\alpha = 0$), is the same as the energy used for the geodesic active contour model, but there is a scale factor of $1/L$. This removes the length shrinking effect of (15) in descent flows; in particular if there are no edges (ϕ is constant), then a descent flow will not shrink the contour. The $\mathbb{L}^2$ gradient of the first term (when $\alpha = 0$ in (16)) as noted in (2) is $-L(\phi - \overline{\phi})\kappa\mathcal{N} + L(\nabla\phi \cdot \mathcal{N})\mathcal{N}$, which is zero when the contour is aligned on true edges of the image (note that this may not be the case with the geodesic active contour model). The flow is stable with respect to the Sobolev metric, but not with respect to $\mathbb{L}^2$.

Dividing the energy (15) by L, as in the first term of (16), loses regularizing effects of the original flow, and it is possible that the contour can become non-smooth from irrelevant noise. This observation is the reason for the second term of (16). The second term, $L \int_c \phi \kappa^2 \, \mathrm{d}s$, is an image dependent version of the scale-invariant elastic energy. This term favors smooth contours, but smoothness is relaxed in the presence of edges, which are determined by ϕ. The factor of L makes the energy scale-invariant when ϕ is constant; therefore, a descent flow will not increase or decrease the length of the contour unless these behaviors make the curvature smaller or make the contour align along the edges. The reason for not considering this term alone is for the following reason. Suppose we are considering open curves with two endpoints fixed. Regardless of the ϕ that is chosen, the minimum of this term is always zero, and it is minimized by a straight line (the curvature is zero). For closed contours, we have observed in the numerical implementation that the contour sticks to isolated points where there is an edge of the image, and the converged contour is a straight line between these points (even if there is no edge along the line). Thus, the contour looks polygon-like. Even though the $\kappa = +\infty$ at vertices of polygons, this is not true numerically where κ is finite. Therefore, in a numerical implementation, the second term of (16) is not useful by itself.

4.2 Increasing Weighted Length

Instead of a non-shrinking edge-based model, if we have prior information that the length of the curve should increase, *e.g.*, the initial curve is within the object of interest, then one may want to *maximize* the following energy:

$$E(c) = \int_c \phi(c(s))\,\mathrm{d}s - \alpha \int_c \kappa^2(s)\,\mathrm{d}s \tag{17}$$

where $\alpha \geq 0$, and ϕ, contrary to the geodesic active contour model, is designed to be large near edges (one example is choosing $\phi = \|\nabla I\|$). The first term of the energy is weighted length, and therefore this term favors increasing the length of the curve while stopping near edges. Considering only the first term ((17) when $\alpha = 0$), since the length of the curve is being increased, it is likely that when the curve has converged on a coarse scale, fine details due to noise become detected and the curve becomes rough, thereby further increasing length. Therefore, we add a regularizer, which is the second term of (17), to the weighted length. Note that we propose to use the scale-varying elastic energy, which in addition to regularity, gives an effect of increasing the length of curve, which is beneficial based on the prior assumption.

The $\mathbb{L}^2$ gradient ascent of the weighted length term results in one term that is $-\phi\kappa\mathcal{N}$, which makes the length of the curve increase and is unstable. If $\alpha > 0$, then the $\mathbb{L}^2$ flow of (17) may become well-posed since this results in higher order regularity terms, but the elastic energy has its own problems using the $\mathbb{L}^2$ gradient flow. Therefore, we use the Sobolev flow.

5 Experiments

5.1 Regularity of Sobolev Active Contour

In this experiment, we show a case when the scale-invariant elastic regularity term (11) is more beneficial than the using the traditional length penalty (9). Note that the elastic regularizer does not generally have a length shrinking effect, but keeps the contour regular. This length shrinking effect may have a detrimental effect as shown in Fig. 1. Note that the length penalty restricts the curve from moving into the groves between the fingers. The elastic regularity term, on the other hand, has no such restriction, and makes the curve more smooth and rounded.

5.2 Tracking with Centroid/ Isoperimetric Prior

In this experiment, we illustrate one possible application of the energy (13) in tracking a man through an occlusion. For the data-based term in (13), we use the Mumford-Shah energy [4]. The prior information on the centroid and isoperimetric ratio can be obtained through a filtering process (indeed, we assume a constant acceleration model of both quantities). We use the tracking framework of [28] for both simulations in Fig. 2. The top row shows the result using the framework of [28] without the use of prior centroid and isoperimetric information; the bottom row incorporates this prior information. Notice that the prior information on the centroid keeps the contour moving through the occlusion, while the isoperimetric ratio (and because we are using Sobolev active contours) keeps the shape constrained.

5.3 Edge Detection with Non-shrinking Model

In this experiment, we demonstrate that the traditional edge-based geodesic active contour model has an arbitrary length shrinking effect that causes the contour to pass over

Fig. 1. $\mathbb{L}^2$ regularization (top two rows). Left to right: $\alpha = 1000$, $\alpha = 1000$ followed by curvature smoothing to remove the noise (least number of iterations to remove noise), $\alpha = 10000, 50000, 90000$. The image-based term is Chan-Vese. Sobolev elastic regularization (bottom two rows). Left to right: $\alpha = 0, 0.1, 5, 10, 25$. The second and fourth row show the same result as the row above them, but the image is removed for visibility.

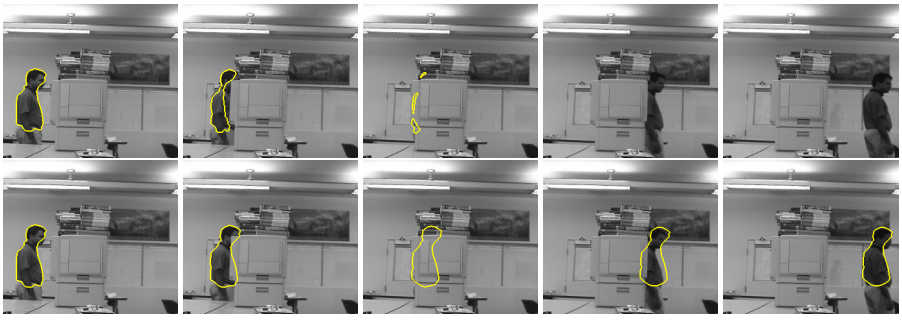

Fig. 2. Tracking a man through an occlusion. Bottom row shows the results of using a prediction (filtering) on the centroid and the isoperimetric ratio, and then penalizing deviations of the contour away from predicted parameters by (13) ($\alpha = 50000$, $\beta = 100$). The top row gives the result with no such penalty. Both use Sobolev active contours.

some meaningful edges. We show that the non-shrinking edge-based model (16) can help correct this behavior. We use edge-map, $1/(1+\phi)$, where

$$\phi(x) = \frac{1}{|B_r|}\int_{B_r(x)} (I(y) - \overline{I}_r(x))^2 \, \mathrm{d}A(y), \text{ where } \overline{I}_r(x) = \frac{1}{|B_r|}\int_{B_r(x)} I(y)\, \mathrm{d}A(y), \tag{18}$$

$B_r(x) = \{y \in \mathbb{R}^2 : \|y - x\| \leq r\}$, and $|B_r|$ denotes the area of B_r.

In Fig. 3, we segment a cyst image using various initializations. Notice that the contour with the traditional edge-based energy (using the $\mathbb{L}^2$ or the Sobolev descents) consistently passes over the edge on the right side of the cyst. The non-shrinking model consistently captures the correct segmentation.

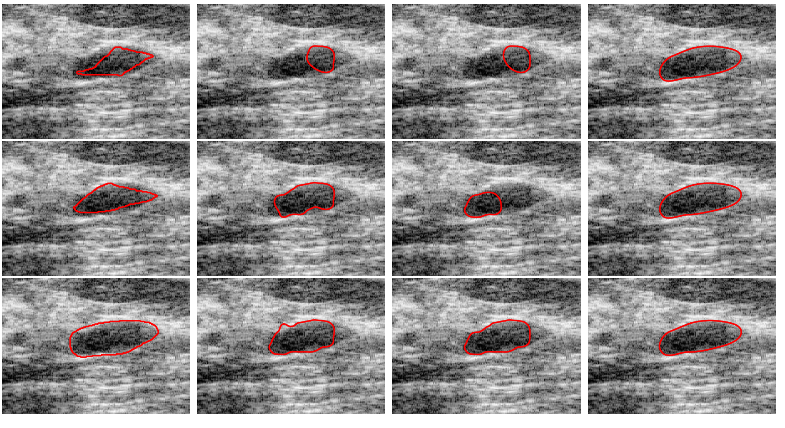

Fig. 3. Segmentation of cyst image with three different initializations (first image in each row). Converged results for the (15) and $\mathbb{L}^2$ active contour (second image), (15) with the Sobolev active contour (third image), and the energy (16) (last image).

5.4 Edge Detection by Increasing Weighted Length

In this experiment, we apply the weighted length increasing energy (17) to vessel segmentation. We show the results of using the traditional edge-based technique with a balloon; that is, we show results of using the $\mathbb{L}^2$ gradient descent for the energy

$$E(c) = \int_c \phi(c(s))\, \mathrm{d}s - \alpha \int_R \phi \, \mathrm{d}A. \tag{19}$$

We use (18) as the edge-map for the weighted length increasing flow. The edge-map for (19) is $1/(1+\phi)$ where ϕ is given in (18).

In the case of vessel segmentation, it beneficial to increase the length of the initial contour more so than area. Since a vessel is characterized as a long, thin structure, a balloon term will fail to capture the global geometry of the vessel. This is demonstrated in Fig. 4: a small weight on the balloon term results in the flow capturing local features close to the initial contour; larger weights on the balloon makes the contour balloon out

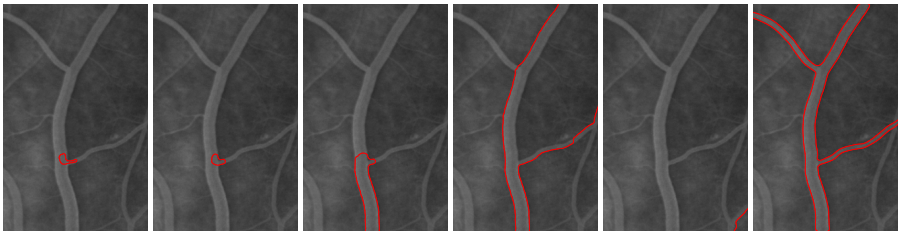

Fig. 4. Left to right: initial contour, minimizing (19) $\alpha = 0.2, 0.25, 0.4$ using $\mathbb{L}^2$, and increasing weighted length (17) $\alpha = 0.1$ using Sobolev (all images show converged contour). The contour expands to enclose the entire image (fifth image).

to capture the entire image. Note the weighted length maximizing flow does not pass the walls of the vessel since that does not increase the *length* (although it does increase area) of the contour, and is therefore able to capture the vessel.

6 Conclusion

We have demonstrated that the Sobolev gradient method allows one to consider active contour energies that were not considered in the past because the gradient method using the traditional metric cannot be used. In particular, we have given examples of energies that result in $\mathbb{L}^2$ gradients that are ill-posed or high order PDEs (and hence numerically difficult to implement). These energies, as we have shown, result in Sobolev gradient flows that are both well-posed and numerically simple to implement. The experiments have shown potential uses for some energies introduced in segmentation and tracking applications.

References

1. Kass, M., Witkin, A., Terzopoulos, D.: Snakes: Active contour models. International Journal of Computer Vision **1** (1987) 321–331
2. Caselles, V., Kimmel, R., Sapiro, G.: Geodesic active contours. In: Proceedings of the IEEE Int. Conf. on Computer Vision, Cambridge, MA, USA (1995) 694–699
3. Kichenassamy, S., Kumar, A., Olver, P., Tannenbaum, A., Yezzi, A.: Gradient flows and geometric active contour models. In: Proceedings of the IEEE Int. Conf. on Computer Vision. (1995) 810–815
4. Mumford, D., Shah, J.: Optimal approximations by piecewise smooth functions and associated variational problems. Comm. Pure Appl. Math. **42** (1989) 577–685
5. Chan, T., Vese, L.: Active contours without edges. IEEE Transactions on Image Processing **10**(2) (2001) 266–277
6. Chen, Y., Tagare, H., Thiruvenkadam, S., Huang, F., Wilson, D., Gopinath, K., Briggs, R., Geiser, E.: Using prior shapes in geometric active contours in a variational framework. International Journal of Computer Vision **50**(3) (2002) 315–328
7. Rousson, M., Paragios, N.: Shape priors for level set representations. In: Proc. European Conf. Computer Vision. Volume 2. (2002) 78–93

8. Cremers, D., Soatto, S.: A pseudo distance for shape priors in level set segmentation. In: IEEE Int. Workshop on Variational, Geometric and Level Set Methods. (2003) 169–176
9. Kim, J., Fisher, J., Yezzi, A., Cetin, M., Willsky, A.: Nonparametric methods for image processing using information theory and curve evolution. In: IEEE International Conference on Image Processing. Volume 3. (2002) 797–800
10. Rochery, M., Jermyn, I., Zerubia, J.: Higher order active contours and their application to the detection of line networks in satellite imagery. In: IEEE Workshop on VLSM. (2003)
11. Sundaramoorthi, G., Yezzi, A.J.: More-than-topology-preserving flows for active contours and polygons. In: ICCV. (2005) 1276–1283
12. Cohen, L.D., Kimmel, R.: Global minimum for active contour models: A minimal path approach. In: CVPR. (1996) 666–673
13. Boykov, Y., Jolly, M.P.: Interactive graph cuts for optimal boundary and region segmentation of objects in n-d images. In: ICCV. (2001) 105–112
14. Kolmogorov, V., Boykov, Y.: What metrics can be approximated by geo-cuts, or global optimization of length/area and flux. In: ICCV. (2005) 564–571
15. Michor, P., Mumford, D.: Riemannian geometries on the space of plane curves. ESI Preprint 1425, arXiv:math.DG/0312384 (2003)
16. Yezzi, A.J., Mennucci, A.: Conformal metrics and true "gradient flows" for curves. In: ICCV. (2005) 913–919
17. Sundaramoorthi, G., Yezzi, A., Mennucci, A.: Sobolev active contours. In: VLSM. (2005) 109–120
18. Charpiat, G., Keriven, R., Pons, J., Faugeras, O.: Designing spatially coherent minimizing flows for variational problems based on active contours. In: ICCV. (2005)
19. Sundaramoorthi, G., Jackson, J.D., Yezzi, A.J., Mennucci, A.: Tracking with sobolev active contours. In: CVPR (1). (2006) 674–680
20. Horn, B.K.P.: The curve of least energy. ACM Transactions on Mathematical Software **9**(4) (1983) 441–460
21. Bruckstein, A.M., Netravali, A.N.: On minimal energy trajectories. Comput. Vision Graph. Image Process. **49**(3) (1990) 283–296
22. Polden, A.: Curves and Surfaces of Least Total Curvature and Fourth-Order Flows. PhD thesis, Mathematisches Institut Unversitat Tubingen, Germany (1996)
23. Sapiro, G., Tannenbaum, A.: Area and length preserving geometric invariant scale-spaces. IEEE Trans. Pattern Anal. Mach. Intell. **17**(1) (1995) 67–72
24. Delingette, H.: On smoothness measures of active contours and surfaces. In: VLSM '01: Proceedings of the IEEE Workshop on Variational and Level Set Methods (VLSM'01), Washington, DC, USA, IEEE Computer Society (2001) 43
25. Brook, A., Bruckstein, A.M., Kimmel, R.: On similarity-invariant fairness measures. In: Scale-Space. (2005) 456–467
26. Ma, T., Tagare, H.: Consistency and stability of active contours with euclidean and non-euclidean arc lengths. IEEE Transactions on Image Processing **8**(11) (1999) 1549–1559
27. Fua, P., Leclerc, Y.G.: Model driven edge detection. Mach. Vision Appl. **3**(1) (1990) 45–56
28. Jackson, J., Yezzi, A., Soatto, S.: Tracking deformable moving objects under severe occulsions. In: IEEE Conference on Decision and Control. (2004)